

Deep Active Learning: Unified and Principled Method for Query and Training

Changjian Shui¹Fan Zhou¹Christian Gagné^{1,2}Boyu Wang^{3,4}¹Université Laval ²Mila, Canada CIFAR AI Chair ³University of Western Ontario ⁴Vector Institute

Abstract

In this paper, we are proposing a unified and principled method for both the querying and training processes in deep batch active learning. We are providing theoretical insights from the intuition of modeling the interactive procedure in active learning as distribution matching, by adopting the Wasserstein distance. As a consequence, we derived a new training loss from the theoretical analysis, which is decomposed into optimizing deep neural network parameters and batch query selection through alternative optimization. In addition, the loss for training a deep neural network is naturally formulated as a min-max optimization problem through leveraging the unlabeled data information. Moreover, the proposed principles also indicate an *explicit* uncertainty-diversity trade-off in the query batch selection. Finally, we evaluate our proposed method on different benchmarks, consistently showing better empirical performances and a better time-efficient query strategy compared to the baselines.

1 Introduction

Deep neural networks (DNNs) achieved unprecedented success for many supervised learning tasks such as image classification and object detection. Although DNNs are successful in many scenarios, there still exists an obvious limitation: the requirement for a large set of labeled data. To address this issue, *Active Learning* (AL) appears as a compelling solution by searching the most informative data points (batch) to label from a pool of unlabeled samples in order to maximize prediction performance.

How to search the most informative samples in the context of DNN? A common solution is to apply DNN's output confidence score as an uncertainty acquisition func-

tion to conduct the query [Settles, 2012, Gal et al., 2017, Haussmann et al., 2019]. However, a well-known issue for uncertainty-based sampling in AL is the so-called *sampling bias* [Dasgupta, 2011]: the current labeled points are not representative of the underlying distribution. For example, as shown in Fig. 1, let us assume that the very few initial samples we obtain lie in the two extreme regions. Then based on these initial observations, the queried samples nearest to the currently estimated decision boundary will lead to a final sub-optimal risk of 10% instead of the true optimal risk of 5%. This will be even more severe in high dimensional and complex datasets, which are common when DNNs are employed.

Recent works have considered obtaining a diverse set of samples for training deep learning with a reduced sampling bias. For example, [Sener and Savarese, 2018] constructed the core-sets through solving the K -center problem. But the search procedure itself is still computationally expensive as it requires constructing a large distance matrix from unlabeled samples. More importantly, it might not be a proper choice particularly for a large-scale unlabeled pool and a *small* query batch, where it is hard to cover the entire data [Ash et al., 2019].

Instead of focusing exclusively on either uncertainty or diversity instances when determining the query, following a hybrid strategy can be more appropriate. For example, [Yin et al., 2017] heuristically selected a portion of samples according to the uncertainty score for exploitation and the remaining portion used random sampling for exploration. [Ash et al., 2019] collected samples whose gradients span a diverse set of directions for implicitly considering these two. Since such hybrid strategies empirically showed improved performance, a goal of our paper is to derive the query strategy that explicitly considers the uncertainty-diversity trade-off in a principled way.

Moreover, in the context of deep AL, the available large set of unlabeled samples may be helpful to construct a good feature representation that would potentially allow to improve performance. In order to further promote better results, the question to answer is how we can additionally design a loss for optimizing DNN's weights that would leverage from the unlabeled samples during the training.

To address this question, a promising line of work is to integrate the training with a *deep generative model* which naturally focuses on the unlabeled data information [Goodfellow et al., 2014, Kingma and Welling, 2013]. Only a few works strode in this direction, notably [Sinha et al., 2019] who empirically adopted a β -VAE to construct the latent variables. Then they adopted the intuition from [Gissin and Shalev-Shwartz, 2019] of searching the diverse unlabeled batch for samples that do not look like the labeled samples, through an adversarial training based on the \mathcal{H} -divergence [Ben-David et al., 2010]. In spite of some good performance, this approach still concentrated on empirically designing the training loss, simply adopting the \mathcal{H} -divergence based query strategy. In particular, *the formal justifications still remain elusive, and the \mathcal{H} -divergence may not be a proper metric for measuring the diversity of the query batch* (see Fig. 2), which will be verified in our paper.

In this paper, we are proposing a *unified and principled* approach for *both* a fast querying and a better training procedure in deep AL, relying on the use of labeled and unlabeled examples. We derived the theoretical analysis through modeling the interactive procedure in AL as *distribution matching* by adopting the Wasserstein distance. We also analytically reveal that the Wasserstein distance is better at capturing the diversity, compared with the most common \mathcal{H} -divergence. From the theoretical result, we derived the loss from the distribution matching, which is naturally decomposed into two stages: optimization of DNN parameters and query batch selection, through alternative optimization.

For the stage of training DNN, the derived loss indicates a min-max optimization problem by leveraging the unlabeled data. More precisely, this involves a maximization of the critic function so as to distinguish the labeled and unlabeled empirical distributions based on the Wasserstein distance, while the feature extractor function aims, on the contrary, to confound the distributions (minimization of empirical distribution divergence). In the query stage, the loss for batch selection *explicitly* indicates the uncertainty-diversity trade-off. For the uncertainty, we want to find the samples with low prediction confidence over two different interpretations: the highest least prediction confidence score and the uniform prediction score (Section 3.4). As for the diversity, we want to find the unlabeled batch holding a larger transport cost w.r.t. the labeled set under Wasserstein distance (i.e. not looking like the current labelled ones), which has been shown as a good metric for measuring diversity.

Finally, we tested our proposed method on different benchmarks, showing a consistently improved performance, particularly in the initial training, and a much faster query strategy compared with the baselines. The results reaffirmed the benefits and potential of deriving unified principles for Deep AL. We also hope it will open up a new avenue for rethinking and designing query efficient and principled Deep AL algorithms in the future.

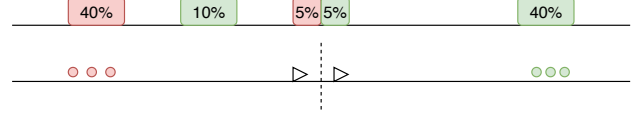


Figure 1: Sampling bias in AL [Dasgupta, 2011]. In the one dimensional binary classification problem (prediction red/green), the data generation distribution consists of four uniform intervals. Red/Green dots: the initial observations; dotted line: estimated decision boundary from the initial samples; triangles: querying samples according to the uncertainty based strategies w.r.t. current decision boundary.

2 Active Learning as Distribution Matching

In supervised learning, observations $\hat{\mathcal{D}}$ are i.i.d. generated by the underlying distribution \mathcal{D} and a labeling function h^* , i.e. $\{(x_i, h^*(x_i))\}_{i=1}^N$ with $x_i \sim \mathcal{D}$. While in AL, the querying sample is not an i.i.d. procedure w.r.t. \mathcal{D} — otherwise it will be simple random sampling. Thus we assume in AL that the query procedure is an i.i.d. empirical process following a distribution $\mathcal{Q} \neq \mathcal{D}$. For example, in the disagreement based approach, \mathcal{Q} can be somehow regarded as a uniform distribution over the disagreement region. Then the interactive procedure can be viewed as estimating a proper \mathcal{Q} to control the generalization error w.r.t. (\mathcal{D}, h^*) .

2.1 Preliminaries

We define the hypothesis $h \in \mathcal{H} : \mathcal{X} \rightarrow \mathcal{Y}$ over $\mathcal{X} \subseteq \mathbb{R}^d$ and $\mathcal{Y} \in [0, 1]$, and loss function $\ell : \mathcal{Y} \times \mathcal{Y} \rightarrow \mathbb{R}^+$. The expected risk w.r.t. \mathcal{D} is $R_{\mathcal{D}}(h) = \mathbb{E}_{x \sim \mathcal{D}} \ell(h(x), h^*(x))$ and empirical risk $\hat{R}_{\mathcal{D}}(h) = \frac{1}{N} \sum_{i=1}^N \ell(h(x_i), y_i)$. $\mathbb{P}(\mathcal{X})$ is the set of all probability measures over \mathcal{X} . We assume that the loss ℓ is symmetric, L -Lipschitz and M -upper bounded and $\forall h \in \mathcal{H}$ is at most H -Lipschitz function.

Wasserstein Distance Given two probability measures $\mathcal{D} \in \mathbb{P}(\mathcal{X})$ and $\mathcal{Q} \in \mathbb{P}(\mathcal{X})$, the *optimal transport* (or Monge-Kantorovich) problem can be defined as searching for a probabilistic coupling (joint probability distribution) $\gamma \in \mathbb{P}(\Omega \times \Omega)$ for $x_{\mathcal{D}} \sim \mathcal{D}$ and $x_{\mathcal{Q}} \sim \mathcal{Q}$ that are minimizing the cost of transport w.r.t. some cost function c :

$$\begin{aligned} & \arg\min_{\gamma} \int_{\mathcal{X} \times \mathcal{X}} c(x_{\mathcal{D}}, x_{\mathcal{Q}})^p d\gamma(x_{\mathcal{D}}, x_{\mathcal{Q}}), \\ & \text{s.t. } \mathbf{P}^+ \# \gamma = \mathcal{D}; \quad \mathbf{P}^- \# \gamma = \mathcal{Q}, \end{aligned}$$

where \mathbf{P}^+ and \mathbf{P}^- is the marginal projection over $\Omega \times \Omega$ and $\#$ denotes the push-forward measure. The p -Wasserstein distance between \mathcal{D} and \mathcal{Q} for any $p \geq 1$ is defined as:

$$W_p^p(\mathcal{D}, \mathcal{Q}) = \inf_{\gamma \in \Pi(\mathcal{D}, \mathcal{Q})} \int_{\mathcal{X} \times \mathcal{X}} c(x_{\mathcal{D}}, x_{\mathcal{Q}})^p d\gamma(x_{\mathcal{D}}, x_{\mathcal{Q}}),$$

where $c : \mathcal{X} \times \mathcal{X} \rightarrow \mathbb{R}^+$ is the cost function of transportation of one unit of mass x to y and $\Pi(\mathcal{D}, \mathcal{Q})$ is the collection of

all joint probability measures on $\mathcal{X} \times \mathcal{X}$ with marginals \mathcal{D} and \mathcal{Q} . Throughout this paper, we only consider the case of $p = 1$, i.e. the Wasserstein-1 distance and the cost function as Euclidean (ℓ_2) distance.

Labeling Function Assumption Some theoretical works show that AL cannot improve the sample complexity in the worst case, thus identifying properties of the AL paradigm is beneficial [Urner and Ben-David, 2013]. For example, [Urner et al., 2013] defined a formal *Probabilistic Lipschitz* condition, in which the Lipschitzness condition is relaxed and formalizes the intuition that *under suitable feature representation, the probability of two close points having different labels is small* [Urner and Ben-David, 2013]. We adopt the Joint Probabilistic Lipschitz property, which can be viewed as an extension of [Pentina and Ben-David, 2018] and is also coherent with [Courty et al., 2017].

Definition 1. Let $\phi : \mathbb{R} \rightarrow [0, 1]$. We say labeling function h^* is $\phi(\lambda)$ -(\mathcal{D}, \mathcal{Q}) Joint Probabilistic Lipschitz if $\text{supp}(\mathcal{Q}) \subseteq \text{supp}(\mathcal{D})$ and for all $\lambda > 0$ and all distribution coupling $\gamma \in \Pi(\mathcal{D}, \mathcal{Q})$:

$$\mathbb{P}_{(x_{\mathcal{D}}, x_{\mathcal{Q}}) \sim \gamma} [|h^*(x_{\mathcal{D}}) - h^*(x_{\mathcal{Q}})| > \lambda \|x_{\mathcal{D}} - x_{\mathcal{Q}}\|_2] \leq \phi(\lambda), \quad (1)$$

where $\phi(\lambda)$ reflects the decay property. [Urner et al., 2013] showed that the faster the decay of $\phi(\lambda)$ with $\lambda \rightarrow 0$, the better the labeling function and the easier it is to learn the task.

2.2 Bound related Querying Distribution

In this part, we will derive the relation between the querying and the data generation distribution.

Theorem 1. Supposing \mathcal{D} is the data generation distribution and \mathcal{Q} is the querying distribution. If the loss ℓ is symmetric, L -Lipschitz; $\forall h \in \mathcal{H}$ is at most H -Lipschitz function and the underlying labeling function h^* is $\phi(\lambda)$ -(\mathcal{D}, \mathcal{Q}) Joint Probabilistic Lipschitz; then the expected risk w.r.t. \mathcal{D} can be upper bounded by:

$$R_{\mathcal{D}}(h) \leq R_{\mathcal{Q}}(h) + L(H + \lambda)W_1(\mathcal{D}, \mathcal{Q}) + L\phi(\lambda). \quad (2)$$

See the proof in the supplementary material. From Eq. (2), the expected risk of \mathcal{D} is upper bounded by the expected risk w.r.t. the query distribution \mathcal{Q} , the Wasserstein distance $W_1(\mathcal{D}, \mathcal{Q})$, and the labeling function property $\phi(\lambda)$. That means a desirable query should hold a small expected risk with a better matching the original distribution \mathcal{D} (diversity).

Non-Asymptotic Analysis Moreover, we can extend the non-asymptotic analysis of Theorem 1 since we generally have finite observations. The proof is also provided in the supplementary material.

Corollary 1. Supposing we have the finite observations which are i.i.d. generated from \mathcal{D} and \mathcal{Q} : $\hat{\mathcal{D}} =$

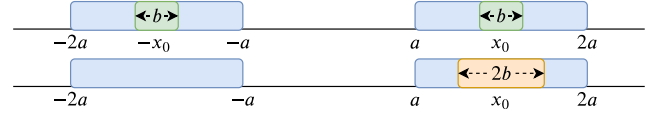


Figure 2: \mathcal{H} -divergence vs. Wasserstein distance for \mathcal{D} - \mathcal{Q} distribution matching. The desirable query distribution should be more diverse (first row) for avoiding *sampling bias* (second row). The computational result shows that \mathcal{H} -divergence is not a proper metric to measure query diversity while Wasserstein is.

$\frac{1}{N} \sum_{i=1}^N \delta\{x_{\mathcal{D}}^i\}$ and $\hat{\mathcal{Q}} = \frac{1}{N_q} \sum_{i=1}^{N_q} \delta\{x_{\mathcal{Q}}^i\}$ with $N_q \leq N$. Then with probability $\geq 1 - \delta$, the expected risk w.r.t. \mathcal{D} can be further upper bounded by:

$$R_{\mathcal{D}}(h) \leq \hat{R}_{\mathcal{Q}}(h) + L(H + \lambda)W_1(\hat{\mathcal{D}}, \hat{\mathcal{Q}}) + L\phi(\lambda) + 2L\text{Rad}_{N_q}(h) + \kappa(\delta, N, N_q),$$

where $\kappa(\delta, N, N_q) = \mathcal{O}(N^{-1/s_d} + N_q^{-1/s_q} + \sqrt{\frac{\log(1/\delta)}{N}} + \sqrt{\frac{\log(1/\delta)}{N_q}})$ with some positive constants s_d and s_q . $\text{Rad}_{N_q}(h) = \mathbb{E}_{S \sim \mathcal{Q}^{N_q}} \mathbb{E}_{\sigma_1^{N_q}} [\sup_h \frac{1}{N_q} \sum_{i=1}^{N_q} \sigma_i h(x_i)]$ is the expected Rademacher complexity generally with $\text{Rad}_{N_q}(h) = \mathcal{O}(\sqrt{\frac{1}{N_q}})$ (e.g [Mohri et al., 2018]).

2.3 Why Wasserstein Distance

In the context of deep active learning, current work such as [Gissin and Shalev-Shwartz, 2019, Sinha et al., 2019] generally explicitly or implicitly adopted the idea of \mathcal{H} -divergence [Ben-David et al., 2010]: $d_{\mathcal{H}}(\mathcal{D}, \mathcal{Q}) = 1 - 2\epsilon$, with ϵ the prediction error when training a binary classifier to *discriminate* the observations sampling from the query and original distribution. Thus a smaller error facilitates the separation of the two distributions with larger \mathcal{H} -divergence and vice versa.

However, we should notice that in AL, $\text{supp}(\mathcal{Q}) \subseteq \text{supp}(\mathcal{D})$, thus \mathcal{H} -divergence may not be a good metric for indicating the diversity property of the querying distribution. On the contrary, Wasserstein distance reflects an optimal transport cost for moving one distribution to another. A smaller transport cost means a better coverage of the distribution \mathcal{D} .

For a better understanding of this problem, we give an illustrative example by computing the exact \mathcal{H} -divergence and Wasserstein-1 distance in one-dimension, shown in Fig. 2. More specifically, we have three uniform distributions: \mathcal{D}_1 the original data distribution, $\mathcal{D}_2, \mathcal{D}_3$ two different query

distributions:

$$\begin{aligned}\mathcal{D}_1 &\sim \mathcal{U}([-2a, -a] \cup [a, 2a]), \\ \mathcal{D}_2 &\sim \mathcal{U}([-x_0 - \frac{b}{2}, -x_0 + \frac{b}{2}] \cup [x_0 - \frac{b}{2}, x_0 + \frac{b}{2}]), \\ \mathcal{D}_3 &\sim \mathcal{U}([x_0 - b, x_0 + b]).\end{aligned}$$

In AL, we can further assume $\text{supp}(\mathcal{D}_2) \subseteq \text{supp}(\mathcal{D}_1)$, $\text{supp}(\mathcal{D}_3) \subseteq \text{supp}(\mathcal{D}_1)$ and $a > b > 0$. For \mathcal{H} -divergence, we set the classifier as a threshold function $f(x) = \mathbf{1}\{x \geq p\}$. Then we can compute the exact $d_{\mathcal{H}}(\cdot, \cdot)$ and $W_1(\cdot, \cdot)$:

$$\begin{aligned}d_{\mathcal{H}}(\mathcal{D}_1, \mathcal{D}_2) &= d_{\mathcal{H}}(\mathcal{D}_1, \mathcal{D}_3) \\ \min_{x_0} W_1(\mathcal{D}_1, \mathcal{D}_3) &> \max_{x_0} W_1(\mathcal{D}_1, \mathcal{D}_2)\end{aligned}\quad (3)$$

From Eq. (3), the \mathcal{H} -divergence indicates the same divergence result where Wasserstein-1 distance exactly captures the property of diversity: *more diverse query distribution \mathcal{Q} means smaller Wasserstein-1 distance $W_1(\mathcal{D}, \mathcal{Q})$.*

3 Practical Deep Batch Active Learning

We have discussed the interactive procedure as the distribution matching and also showed that Wasserstein distance is a *proper* metric for measuring the diversity during distribution matching. Based on the aforementioned analysis, in the batch active learning problem, we have labelled data $\hat{L} = \frac{1}{L} \sum_{i=1}^L \delta\{x_i^l\}$ and its labels $\{y_i^l\}_{i=1}^L$, unlabelled data $\hat{U} = \frac{1}{U} \sum_{i=1}^U \delta\{x_i^u\}$ and total distribution $\hat{\mathcal{D}} = \hat{L} \cup \hat{U}$ with partial labels $\{y_i^l\}_{i=1}^L$. The goal of AL at each interaction is: 1) find a batch $\hat{B} = \frac{1}{B} \sum_{i=1}^B \delta\{x_i^b\}$ with $x_i^b \in \hat{U}$ during the query; 2) find a hypothesis $h \in \mathcal{H}$ such that:

$$\min_{\hat{B}, h} \hat{R}_{\hat{L} \cup \hat{B}}(h) + \mu W_1(\hat{\mathcal{D}}, \hat{L} \cup \hat{B}). \quad (4)$$

Eq.(4) follows the principles (upper bound) from Theorem 1 and Corollary 1. Moreover, if we fix the hypothesis h , the sampled batch holds the following two requirements simultaneously:

1. Minimize the empirical error. We will show later it is related to uncertainty based sampling.
2. Minimize the Wasserstein-1 distance w.r.t. original distribution, which encourages a better distribution matching of $\hat{\mathcal{D}}$.

3.1 Min-Max Problem in DNN

Based on Eq.(4), we can extend the loss to the deep representation learning scenario, since directly estimating the Wasserstein-1 distance through solving optimal transport for complex and large-scale data is still a challenging and open problem. Then inspired by [Arjovsky et al., 2017], we

then adopt the min-max optimizing through training the DNN. Namely, according to Kantorovich-Rubinstein duality, Eq. (4) can be reformulated as:

$$\min_{\theta^f, \theta^h, \hat{B}} \max_{\theta^d} \hat{R}(\theta^f, \theta^h) + \mu \hat{E}(\theta^f, \theta^d), \quad (5)$$

where $\theta^f, \theta^h, \theta^d$ are parameters corresponding to the *feature extractor*, *task predictor* and *distribution critic*; \hat{R} is the predictor loss and \hat{E} is the adversarial (min-max) loss.

We further denote the *parametric task prediction* function $h(x, y, (\theta^f, \theta^h)) \equiv h(x, y) : \mathcal{X} \times \mathcal{Y} \rightarrow (0, 1]$ with $\sum_y h(x, y) = 1$ and the *parametric critic* function $g(x, (\theta^f, \theta^d)) \equiv g(x) : \mathcal{X} \rightarrow [0, 1]$ with restricting $g(x)$ to the 1-Lipschitz function (Kantorovich-Rubinstein theorem). Then each term in Eq. (5) can be expressed as:

$$\begin{aligned}\hat{R}(\theta^f, \theta^h) &= \mathbb{E}_{(x, y) \sim \hat{L} \cup \hat{B}} \ell(h(x, y)), \\ \hat{E}(\theta^f, \theta^d) &= \mathbb{E}_{x \sim \hat{\mathcal{D}}} [g(x)] - \mathbb{E}_{x \sim \hat{L} \cup \hat{B}} [g(x)].\end{aligned}$$

3.2 Two-stage Optimization

Then through some computation, we can decompose Eq. (5) into three terms:

$$\begin{aligned}&\min_{\theta^f, \theta^h, \hat{B}} \max_{\theta^d} \underbrace{\frac{1}{L+B} \sum_{(x, y) \in \hat{L}} \ell(h(x, y))}_{\text{Training: Prediction Loss}} \\ &+ \underbrace{\mu \left(\frac{1}{L+U} \sum_{x \in \hat{U}} g(x) - \left(\frac{1}{L+B} - \frac{1}{L+U} \right) \sum_{x \in \hat{L}} g(x) \right)}_{\text{Training: Min-max Loss}} \\ &+ \underbrace{\frac{1}{L+B} \sum_{(x, y^?) \in \hat{B}} \ell(h(x, y^?)) - \frac{\mu}{L+B} \sum_{x \in \hat{B}} g(x)}_{\text{Query}},\end{aligned}\quad (6)$$

where the critic function $g(x)$ is 1-Lipschitz and L, U, B are the size of labeled, unlabeled, and query data. $y^?$ is called the *agnostic-label*, since it is not available during the query stage. Then from Eq. (6), each interaction of AL can be naturally decomposed into two stages (optimizing DNN and batch selection), through alternative optimization.

3.3 Training DNN

In the training stage, we used all of the observed data to optimize the neural network parameters:

$$\begin{aligned}&\min_{\theta^f, \theta^h} \max_{\theta^d} \frac{1}{L+B} \sum_{(x, y) \in \hat{L}} \ell(h(x, y)) \\ &+ \mu \left(\frac{1}{L+U} \sum_{x \in \hat{U}} g(x) - \left(\frac{1}{L+B} - \frac{1}{L+U} \right) \sum_{x \in \hat{L}} g(x) \right),\end{aligned}\quad (7)$$

with restricting $g(x)$ to the 1-Lipschitz function. Instead of only minimizing the prediction error, the proposed approach naturally leveraged the unlabeled data information through a min-max training. More intuitively, the critic function g aims to evaluate how probable it is that the sample comes from the labeled or unlabeled parts¹. According to the loss, given a fixed g , when $g(x) \rightarrow 1$ meaning that it is highly probable that the samples come from the unlabeled set $x \in \hat{U}$ and vice versa. Since $B < U$, thus $\frac{1}{L+B} - \frac{1}{L+U} > 0$, means the proposed adversarial loss being always valid.

Based on Eq. (7), we call this framework the Wasserstein Adversarial Active Learning (WAAL) in our deep batch AL. The labeled \hat{L} and unlabeled data \hat{U} pass a common feature extractor, then \hat{L} will be used in the prediction and \hat{L}, \hat{U} together will be used in the min-max (adversarial) training. In the practical deep learning, we apply the cross entropy loss: $\ell(x, y) = -\log(h(x, y))^2$.

Redundancy Trick One can directly apply gradient descent to optimize Eq. (7) on the whole dataset. Actually, we generally apply the mini-batch based SGD approach in training the DNN³. While a practical concern during the adversarial training procedure is the unbalanced label and unlabeled data during the training procedure. Thus we propose the *redundancy trick* to solve this concern. For abuse of notation, we denote the unbalanced ratio $\gamma = \frac{U}{L}$ and the query ratio $\alpha = \frac{B}{L}$, with the adversarial loss simplified as:

$$\mu' \left(\frac{1}{U} \sum_{x \in \hat{U}} g(x) - \frac{1}{\gamma} \frac{\gamma - \alpha}{1 + \alpha} \frac{1}{L} \sum_{x \in \hat{L}} g(x) \right),$$

with $\mu' = \frac{\gamma}{1+\gamma} \mu$.

Then following the *redundancy trick* for optimizing the adversarial loss, we keep the same mini-batch size S for labelled and unlabeled observations. Due to the existence of the unbalanced data, we simply conduct a sampling with replacement to construct the training batch for the labeled data, then divided by the unbalanced ratio γ . For each training batch, the adversarial loss can be rewritten as:

$$\min_{\theta^f} \max_{\theta^d} \mu' \left(\frac{1}{S} \sum_{x \in \hat{U}_S} g(x) - C_0 \frac{1}{S} \sum_{x \in \hat{L}_S} g(x) \right), \quad (8)$$

where \hat{U}_s, \hat{L}_s are unlabeled and labeled training batch and $C_0 = \frac{1}{\gamma^2} \frac{\gamma - \alpha}{1 + \alpha}$ is the ‘‘bias coefficient’’ in deep active adversarial training. For example, if there exist 1K labeled

samples, 9K unlabeled samples and a current query batch budget of 1K, then we can compute $C_0 \approx 0.05$ so as to control excessive reusing of the labelled dataset.

3.4 Query Strategy

The second stage over the unlabeled data aims to find a querying batch such that:

$$\operatorname{argmin}_{\hat{B} \subset \hat{U}} \frac{1}{L+B} \sum_{(x, y^?) \in \hat{B}} \ell(h(x, y^?)) - \frac{\mu}{L+B} \sum_{x \in \hat{B}} g(x), \quad (9)$$

where $y^?$ is the agnostic-label.

Agnostic-label upper bound loss indicates uncertainty

Since we do not known $y^?$ during the query, we can instead optimize an *upper bound* of Eq. (9). In the classification problem with cross entropy loss, suppose that we have $\{1, \dots, K\}$ possible outputs with $\sum_{y \in \{1, \dots, K\}} h(x, y) = 1$, then we have upper bounds Eq. (10) and (11), which both reflect the uncertainty measures with different interpretations.

1. Minimizing over the single worst case upper bound indicates the sample with the *highest least prediction confidence score*:

$$\min_x \ell(h(x, y^?)) \leq \min_x \max_{y \in \{1, \dots, K\}} -\log(h(x, y)). \quad (10)$$

For example, we have two samples with a binary decision score $h(x_1, \cdot) = [0.4, 0.6]$ and $h(x_2, \cdot) = [0.3, 0.7]$. Since $\max_y -\log(h(x_1, y)) < \max_y -\log(h(x_2, y))$, we will choose x_1 as the query since the least prediction label confidence 0.4 is higher. Intuitively such a sample seems uncertain since the least label prediction confidence is high⁴.

2. Minimizing over ℓ_1 norm upper bound indicates the sample with a *uniformly of prediction confidence score*:

$$\min_x \ell(h(x, y^?)) \leq \min_x \sum_{y \in \{1, \dots, K\}} -\log(h(x, y)). \quad (11)$$

Intuitively if the sample’s prediction confidence trend is more uniform, the more uncertain the sample will be. We can also show the min arrives when the output score is uniform, as shown in the supplementary material.

We would like to point out that the upper bounds proposed in Eq. (10,11) are additive, i.e. we can apply any convex combination for these two losses as the hybrid uncertain query strategy.

⁴In the binary classification problem, it recovers the least prediction confidence score approach (Baseline 2), which is a common strategy in AL.

¹We should point out that this is the high-level intuition. More specifically, the critic parameter θ^d of g tries to maximize and the feature parameter θ^f of g tries to minimize the adversarial loss according to the Wasserstein metric. Moreover the proposed min-max loss differs from the standard Wasserstein min-max loss since they hold different weights (‘‘bias coefficient’’)

²Although the cross entropy loss does not satisfy the exact assumptions in the theoretical analysis, our later experiments suggest that the proposed algorithm is very effective for cross-entropy loss.

³We have referred to this as the *training/mini batch* to avoid any confusion with the querying batch mentioned before.

Critic output indicates diversity As for the critic function $g(x) : \mathcal{X} \rightarrow [0, 1]$ from the adversarial loss, if the critic function output trends to $g(x) \rightarrow 1$, it means $x \in \hat{U}$ and vice versa. Then according to the query loss, we want to select the batch with higher critic values $g(x)$, meaning they look more different than the labelled samples under the Wasserstein metric.

If the unlabeled samples look like the labeled ones (small $g(x)$ with $x \in \hat{U}$), then under some proper conditions (such as *Probabilistic Lipschitz Condition* in def. 1), such examples can be more easily predicted because we can infer them from their very near neighbours' information.

On the contrary, the unlabeled samples with high $g(x)$ under the current assumption cannot be effectively predicted by the current labeled data (far away data). Moreover, the $g(x)$ is trained through Wasserstein distance based loss, shown as a proper metric for measuring the diversity. Therefore the query batch with higher critic value ($g(x)$) means a larger transport cost from the labeled samples, indicating that it is more informative and represents diversity.

Remark The aforementioned two terms in the query strategy indicate an explicit *uncertainty* and *diversity* trade-off. Uncertainty criteria can reduce the empirical risk but leading to a potential sampling bias. While the diversity criteria can improve the exploration of the distribution while might be inefficient for a small query batch. Our query approach naturally combines these two, for choosing the samples with prediction uncertainty and diversity. Moreover, since Eq. (9) is additive, we can easily estimate the query batch through the greedy algorithm.

3.5 Proposed Algorithm

Based on the previous analysis, our proposed algorithm includes a training stage [Eq. (7,8)] and a query stage [Eq. (9), (10) and (11)] for solving Eq. (5) or (6). We only show the learning algorithm for one interaction in Algorithm 1, then the remaining interactions will be repeated accordingly.

Since the discriminator function g should be restricted in 1-Lipschitz, we add the gradient penalty term such as [Gulrajani et al., 2017] to g to restrict the Lipschitz property.

4 Experiments

We start our experiments with a small initial labeled pool of the training set. The initial observation size and the budget size range from 1% – 5% of the training dataset, depending on the task. Following Alg. 1, the selected batch will be annotated and added into the training set. Then the training process for the next iteration will be repeated on the new formed labeled and unlabeled set *from scratch*.

Algorithm 1 WAAL: one interaction

Require: Labeled samples \hat{L} , unlabeled samples \hat{U} , query budget B and hyper-parameters (learning rate η , trade-off rate μ, μ')

Ensure: Neural network parameters $\theta^f, \theta^h, \theta^d$

- 1: $\triangleright \triangleright \triangleright$ **DNN Parameter Training Stage** $\triangleleft \triangleleft \triangleleft$
- 2: **for** mini-batch of samples $\{(x^u)\}_{i=1}^S$ from \hat{U} **do**
- 3: Constructing mini-batch $\{(x^l, y^l)\}_{i=1}^S$ from \hat{L} through sampling with replacement (redundancy trick).
- 4: Updating θ^h : $\theta^h = \theta^h - \frac{\eta}{S} \sum_{(x^l, y^l)} \frac{\partial \ell(h((x^l, y^l)))}{\partial \theta^h}$
- 5: Updating θ^f : $\theta^f = \theta^f - \frac{\eta}{S} \left(\sum_{(x^l, y^l)} \frac{\partial \ell(h((x^l, y^l)))}{\partial \theta^f} + \mu' \left\{ \sum_{x^u} \frac{\partial g(x)}{\partial \theta^f} - C_0 \sum_{x^l} \frac{\partial g(x)}{\partial \theta^f} \right\} \right)$
- 6: Updating θ^d : $\theta^d = \theta^d + \frac{\eta \mu'}{S} \left\{ \sum_{x^u} \frac{\partial g(x)}{\partial \theta^d} - C_0 \sum_{x^l} \frac{\partial g(x)}{\partial \theta^d} \right\}$
- 7: **end for**
- 8: $\triangleright \triangleright \triangleright$ **Querying Stage** $\triangleleft \triangleleft \triangleleft$
- 9: Applying the convex combination of Eq. (10) and (11) to compute uncertainly score $\mathcal{U}(x^u)$;
Computing diversity score $g(x^u)$;
Ranking the score $\mathcal{U}(x^u) - \mu g(x^u)$ with $x^u \in \hat{U}$, choosing the smallest B samples, forming querying batch \hat{B}

10: $\triangleright \triangleright \triangleright$ **Updating** $\triangleleft \triangleleft \triangleleft$

11: $\hat{L} = \hat{L} \cup \hat{B}, \hat{U} = \hat{U} \setminus \hat{B}$

We evaluate our proposed approach on three object recognition tasks, namely Fashion MNIST (image size: 28×28) [Xiao et al., 2017], SVHN (32×32) [Netzer et al., 2011], CIFAR-10 (32×32) [Krizhevsky et al., 2009]. For each task we split the whole data into training, validation and testing parts. We evaluate the performance of the proposed algorithm for image classification task by computing the prediction accuracy. We repeat all of the experiments 5 times and report the average value. The details of the experimental settings (dataset description, train/validation/test splitting, detailed implementations, hyper-parameter settings and choices) and additional experimental results are provided in the supplementary material.

Baselines We compare the proposed approach with the following baselines: 1) Random sampling; 2) Least confidence [Culotta and McCallum, 2005]; 3) Smallest Margin [Scheffer and Wrobel, 2001]; 4) Maximum-Entropy sampling [Settles, 2012]; 5) K -Median approach [Sener and Savarese, 2018]: choosing the points to be labelled as the cluster centers of K -Median algorithm; 6) Core-set approach [Sener and Savarese, 2018]; 7) Deep Bayesian AL (DBAL) [Gal et al., 2017]; and 8) Deep FoolAL [Mayer and Timofte, 2018].

Implementations For the proposed approach, differing from baselines, we train the DNN from labeled

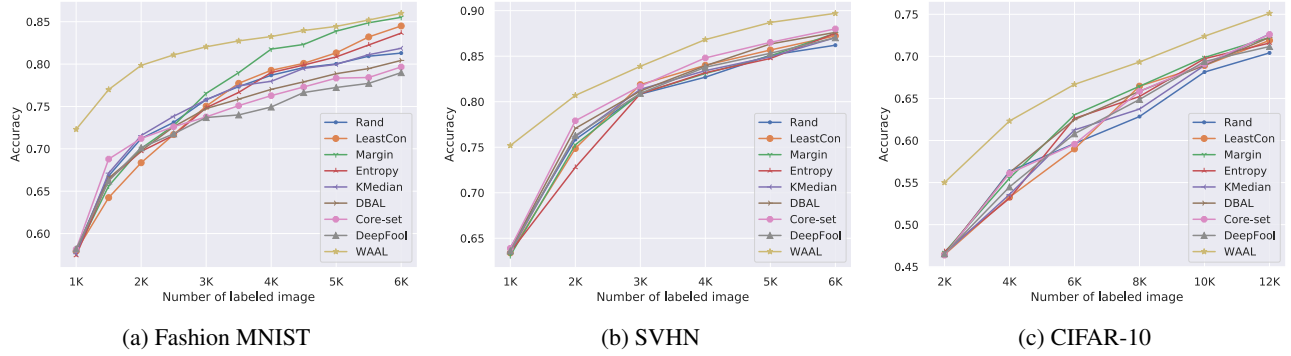


Figure 3: Empirical performance on Fashion MNIST, SVHN and CIFAR-10 over five repetitions.

Method	LeastCon	Margin	Entropy	K -Median	DBAL	Core-set	DeepFool	WAAL
Time	0.94	0.95	0.95	33.98	9.25	45.88	124.46	1

Table 1: Relative Average querying time, assuming the query time of WAAL as the unit.

and unlabeled data without data-augmentation. For the tasks on SVHN, CIFAR-10 we implement VGG16 [Simonyan and Zisserman, 2014] and for task on Fashion MNIST we implement LeNet5 [LeCun et al., 1998] as the feature extractor. On top of the feature extractor, we implement a two-layer multi-layer perceptron (MLP) as the classifier and critic function. For all tasks, at each interaction we set the maximum training epoch as 80. For each epoch, we feed the network with mini-batch of 64 samples and adopt SGD with momentum [Sutskever et al., 2013] to optimize the network. We tune the hyper-parameter through grid search. In addition, in order to avoid over-training, we also adopt early stopping [Caruana et al., 2001] techniques during training.

4.1 Results

We demonstrate the empirical results in Fig. 3. Exact numerical values and standard deviation are reported in the supplementary material. The proposed approach (WAAL) consistently outperforms all of the baselines during the interactions. We noticed that WAAL shows a large improvement ($> 5\%$) in the initial training procedure since it efficiently constructs a good representation through leveraging the unlabeled data information. For the relatively simple input task Fashion MNIST, the simplest uncertainty query (Smallest Margin/Least Confidence) finally achieved almost the same level performance with WAAL under 6K labeled samples. Moreover, we observed that for the small or middle sized queried batch (0.5K-2K) in the relatively complex dataset (SVHN, CIFAR-10), the baselines show similar results in deep AL, which is coherent with previous observations [Gissin and Shalev-Shwartz, 2019, Ash et al., 2019]. On the contrary, our proposed approach still shows a good improved empirical result, emphasizing the benefits of prop-

erly designing loss for considering the unlabeled data in the context of deep AL.

We also report the average query time for the baselines and proposed approach on SVHN dataset in Tab. 1. The results indicates that WAAL holds the same querying time level with the standard uncertainty based strategies since they are all *end-to-end* strategies without knowing the internal information of the DNN. However some diversity based approaches such as Core-set and K -Median require the computation of the distance in the feature space and finally induce a much longer query time.

4.2 Ablation Study: Advantage of Wasserstein Metric

In this part, we empirically show the advantage of considering the Wasserstein distance by the ablation study. Specifically, for the whole baselines we adopt \mathcal{H} -divergence based adversarial loss for training DNN. That is, we set a discriminator and we used the binary cross entropy (BCE) adversarial loss to discriminate the labeled and unlabeled data [Gissin and Shalev-Shwartz, 2019]. Then in the query we still apply the different baselines strategies to obtain the labels. We tested in the CIFAR-10 dataset and report the performances in Fig. 4. Due to space limit, we present the brief introduction, exact numerical values, and more results in the supplementary material.

From the results, we observed that the gap between the initial training procedure has been reduced from about 8% to 5% because of introducing the adversarial based training. However, our proposed approach (WAAL) still consistently outperforms the baselines. The reason might be that the \mathcal{H} -divergence based adversarial loss is not a good metric for the Deep AL as we formally analyzed before. The results indicate the practical potential of adopting the Wasserstein

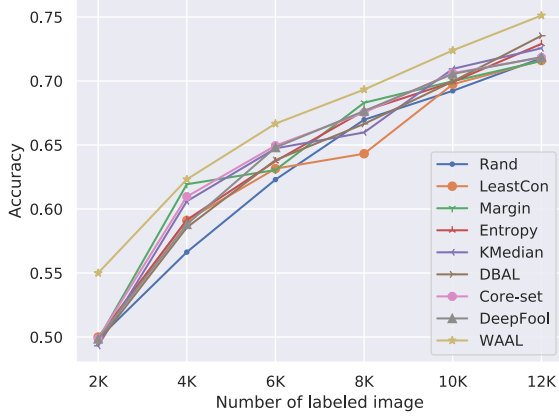


Figure 4: Ablation study in CIFAR-10: the baselines are all trained by leveraging the unlabeled information through \mathcal{H} -divergence.

distance for the Deep AL problem.

5 Related work

Active learning is a long term and promising research topic in theoretical and practical aspects. Here only the most related works are described and interested readers can find further details in the survey papers [Dasgupta, 2011], [Settles, 2012] and [Hanneke et al., 2014]. In the context of deep AL, there are uncertainty and diversity based querying strategies. In the uncertainty based approach, we aim to find the difficult samples by using some heuristics, for example [Gal et al., 2017, Beluch et al., 2018, Haussmann et al., 2019, Pinsler et al., 2019] integrate uncertainty measure with a Bayesian deep neural network; [Ducoffe and Precioso, 2018] adopt adversarial examples as the proxy distance in the margin based approach. In the diversity based query, [Geifman and El-Yaniv, 2017, Sener and Savarese, 2018] apply the Core-set approach for selecting diverse data.

In addition, several works [Guo and Schuurmans, 2008, Wang and Ye, 2015] consider the mixture strategy of combining diversity and uncertainty, which are generally formulated as an iterative optimization problem in the AL, while they are not fit to the usual deep learning scenario. [Bachman et al., 2017] combines the meta-learning with active learning for gradually choosing the proper acquisition function during the interactions. Several papers also adopt the idea of adversarial training (GAN) or variational approach (VAE), such as [Zhu and Bento, 2017, Mayer and Timofte, 2018, Tran et al., 2019]. However they generally simply plug in such generative techniques without analysing the superficiality in the AL.

In the theoretical aspect, different approaches have been proposed such as exploiting the cluster structure through

the hierarchical model, e.g. [Settles, 2012]; or hypothesis space searching through estimating the disagreement region such as [Balcan et al., 2009]. These provable approaches generally provide a strong theoretical guarantee in AL, while they are highly computationally intractable in the DNN scenario.

Distribution Matching is an important research topic in the deep generative model [Goodfellow et al., 2014, Kingma and Welling, 2013] and transfer learning [Ganin et al., 2016, Shui et al., 2019]. In general, it aims at minimizing the statistical divergence between two distributions. In AL, some approaches implicitly connect with distribution matching. [Gissin and Shalev-Shwartz, 2019] investigate \mathcal{H} -divergence between the labeled and unlabeled dataset by constructing a binary classifier, while it has been shown that the \mathcal{H} -divergence is not a proper metric for diversity in AL. [Chattopadhyay et al., 2013, Wang and Ye, 2015, Viering et al., 2017] adopted the Maximum Mean Discrepancy (MMD) metric by constructing a standard optimization problem, which also focuses on query strategy and is not scalable for the complex and large-scale dataset.

6 Conclusion

In this paper, we proposed a unified and principled method for both querying and training in the deep AL. We analyzed the theoretical insights from the intuition of modeling the interactive procedure in AL as distribution matching. Then we derived a new training loss for jointly learning hypothesis and query batch searching. We formulated the loss for DNN as a min-max optimization problem by leveraging the unlabeled data. As for the query for batch selection, it explicitly indicates the uncertainty-diversity trade-off. The results on different benchmarks showed a consistent better accuracy and faster efficient query strategy. The analytical and empirical results reaffirmed the benefits and potentials for reflecting on the unified principles for deep active learning. In the future, we want to 1) understand more general learning scenarios such as different distribution divergence metrics and its corresponding influences; 2) exploring other types of practical principles such as the auto-encoder based approach instead of adversarial training.

7 Acknowledgements

We would like to thank Mahdieh Abbasi and Qi Chen for the insightful discussions and feedback. We also appreciate Annette Schwerdtfeger for proofreading this manuscript. C. Shui and C. Gagné are funded by E Machine Learning, Mitacs, Prompt-Québec, and NSERC-Canada. F. Zhou is supported by China Scholarship Council. B. Wang is supported by the Faculty of Science at the University of Western Ontario.

References

- [Arjovsky et al., 2017] Arjovsky, M., Chintala, S., and Bottou, L. (2017). Wasserstein gan. *arXiv preprint arXiv:1701.07875*.
- [Ash et al., 2019] Ash, J. T., Zhang, C., Krishnamurthy, A., Langford, J., and Agarwal, A. (2019). Deep batch active learning by diverse, uncertain gradient lower bounds. *arXiv preprint arXiv:1906.03671*.
- [Bachman et al., 2017] Bachman, P., Sordoni, A., and Trischler, A. (2017). Learning algorithms for active learning. In *Proceedings of the 34th International Conference on Machine Learning-Volume 70*, pages 301–310. JMLR.org.
- [Balcan et al., 2009] Balcan, M.-F., Beygelzimer, A., and Langford, J. (2009). Agnostic active learning. *Journal of Computer and System Sciences*, 75(1):78–89.
- [Beluch et al., 2018] Beluch, W. H., Genewein, T., Nürnberger, A., and Köhler, J. M. (2018). The power of ensembles for active learning in image classification. In *Proceedings of the IEEE Conference on Computer Vision and Pattern Recognition*, pages 9368–9377.
- [Ben-David et al., 2010] Ben-David, S., Blitzer, J., Crammer, K., Kulesza, A., Pereira, F., and Vaughan, J. W. (2010). A theory of learning from different domains. *Machine learning*, 79(1-2):151–175.
- [Bolley et al., 2007] Bolley, F., Guillin, A., and Villani, C. (2007). Quantitative concentration inequalities for empirical measures on non-compact spaces. *Probability Theory and Related Fields*, 137(3-4):541–593.
- [Caruana et al., 2001] Caruana, R., Lawrence, S., and Giles, C. L. (2001). Overfitting in neural nets: Backpropagation, conjugate gradient, and early stopping. In *Advances in neural information processing systems*, pages 402–408.
- [Chattopadhyay et al., 2013] Chattopadhyay, R., Wang, Z., Fan, W., Davidson, I., Panchanathan, S., and Ye, J. (2013). Batch mode active sampling based on marginal probability distribution matching. *ACM Transactions on Knowledge Discovery from Data (TKDD)*, 7(3):13.
- [Coates et al., 2011] Coates, A., Ng, A., and Lee, H. (2011). An analysis of single-layer networks in unsupervised feature learning. In *Proceedings of the fourteenth international conference on artificial intelligence and statistics*, pages 215–223.
- [Courty et al., 2017] Courty, N., Flamary, R., Habrard, A., and Rakotomamonjy, A. (2017). Joint distribution optimal transportation for domain adaptation. In Guyon, I., Luxburg, U. V., Bengio, S., Wallach, H., Fergus, R., Vishwanathan, S., and Garnett, R., editors, *Advances in Neural Information Processing Systems 30*, pages 3730–3739. Curran Associates, Inc.
- [Culotta and McCallum, 2005] Culotta, A. and McCallum, A. (2005). Reducing labeling effort for structured prediction tasks. In *AAAI conference on artificial intelligence*.
- [Dasgupta, 2011] Dasgupta, S. (2011). Two faces of active learning. *Theoretical computer science*, 412(19):1767–1781.
- [Ducoffe and Precioso, 2018] Ducoffe, M. and Precioso, F. (2018). Adversarial active learning for deep networks: a margin based approach. *CoRR*, abs/1802.09841.
- [Gal et al., 2017] Gal, Y., Islam, R., and Ghahramani, Z. (2017). Deep bayesian active learning with image data. In *Proceedings of the 34th International Conference on Machine Learning-Volume 70*, pages 1183–1192. JMLR.org.
- [Ganin et al., 2016] Ganin, Y., Ustinova, E., Ajakan, H., Germain, P., Larochelle, H., Laviolette, F., Marchand, M., and Lempitsky, V. (2016). Domain-adversarial training of neural networks. *The Journal of Machine Learning Research*, 17(1):2096–2030.
- [Geifman and El-Yaniv, 2017] Geifman, Y. and El-Yaniv, R. (2017). Deep active learning over the long tail. *arXiv preprint arXiv:1711.00941*.
- [Gissin and Shalev-Shwartz, 2019] Gissin, D. and Shalev-Shwartz, S. (2019). Discriminative active learning. *CoRR*, abs/1907.06347.
- [Goodfellow et al., 2014] Goodfellow, I., Pouget-Abadie, J., Mirza, M., Xu, B., Warde-Farley, D., Ozair, S., Courville, A., and Bengio, Y. (2014). Generative adversarial nets. In *Advances in neural information processing systems*, pages 2672–2680.
- [Gulrajani et al., 2017] Gulrajani, I., Ahmed, F., Arjovsky, M., Dumoulin, V., and Courville, A. C. (2017). Improved training of wasserstein gans. In *Advances in Neural Information Processing Systems*, pages 5767–5777.
- [Guo and Schuurmans, 2008] Guo, Y. and Schuurmans, D. (2008). Discriminative batch mode active learning. In *Advances in neural information processing systems*, pages 593–600.
- [Hanneke et al., 2014] Hanneke, S. et al. (2014). Theory of disagreement-based active learning. *Foundations and Trends® in Machine Learning*, 7(2-3):131–309.
- [Haussmann et al., 2019] Haussmann, M., Hamprecht, F., and Kandemir, M. (2019). Deep active learning with

- adaptive acquisition. In *Proceedings of the Twenty-Eighth International Joint Conference on Artificial Intelligence, IJCAI-19*, pages 2470–2476. International Joint Conferences on Artificial Intelligence Organization.
- [Kingma and Welling, 2013] Kingma, D. P. and Welling, M. (2013). Auto-encoding variational bayes. *arXiv preprint arXiv:1312.6114*.
- [Krizhevsky et al., 2009] Krizhevsky, A. et al. (2009). Learning multiple layers of features from tiny images. Technical report, Citeseer.
- [LeCun et al., 1998] LeCun, Y., Bottou, L., Bengio, Y., Haffner, P., et al. (1998). Gradient-based learning applied to document recognition. *Proceedings of the IEEE*, 86(11):2278–2324.
- [Mayer and Timofte, 2018] Mayer, C. and Timofte, R. (2018). Adversarial sampling for active learning. *arXiv preprint arXiv:1808.06671*.
- [Mohri et al., 2018] Mohri, M., Rostamizadeh, A., and Talwalkar, A. (2018). *Foundations of machine learning*. MIT Press.
- [Netzer et al., 2011] Netzer, Y., Wang, T., Coates, A., Bissacco, A., Wu, B., and Ng, A. Y. (2011). Reading digits in natural images with unsupervised feature learning.
- [Pentina and Ben-David, 2018] Pentina, A. and Ben-David, S. (2018). Multi-task kernel learning based on probabilistic lipschitzness. In *Algorithmic Learning Theory*, pages 682–701.
- [Pinsler et al., 2019] Pinsler, R., Gordon, J., Nalisnick, E., and Hernández-Lobato, J. M. (2019). Bayesian batch active learning as sparse subset approximation. In *Advances in Neural Information Processing Systems*, pages 6356–6367.
- [Scheffer and Wrobel, 2001] Scheffer, T. and Wrobel, S. (2001). Active learning of partially hidden markov models. In *In Proceedings of the ECML/PKDD Workshop on Instance Selection*. Citeseer.
- [Sener and Savarese, 2018] Sener, O. and Savarese, S. (2018). Active learning for convolutional neural networks: A core-set approach. In *International Conference on Learning Representations*.
- [Settles, 2012] Settles, B. (2012). Active learning literature survey. Technical report, University of Wisconsin-Madison Department of Computer Sciences.
- [Shui et al., 2019] Shui, C., Abbasi, M., Robitaille, L.-É., Wang, B., and Gagné, C. (2019). A principled approach for learning task similarity in multitask learning. In *Proceedings of the 28th International Joint Conference on Artificial Intelligence*, pages 3446–3452. AAAI Press.
- [Simonyan and Zisserman, 2014] Simonyan, K. and Zisserman, A. (2014). Very deep convolutional networks for large-scale image recognition. *arXiv preprint arXiv:1409.1556*.
- [Sinha et al., 2019] Sinha, S., Ebrahimi, S., and Darrell, T. (2019). Variational adversarial active learning. *arXiv preprint arXiv:1904.00370*.
- [Sutskever et al., 2013] Sutskever, I., Martens, J., Dahl, G., and Hinton, G. (2013). On the importance of initialization and momentum in deep learning. In *International conference on machine learning*, pages 1139–1147.
- [Tran et al., 2019] Tran, T., Do, T.-T., Reid, I., and Carneiro, G. (2019). Bayesian generative active deep learning. In *International Conference on Machine Learning*, pages 6295–6304.
- [Uerner and Ben-David, 2013] Uerner, R. and Ben-David, S. (2013). Probabilistic lipschitzness a niceness assumption for deterministic labels. In *NIPS 2013*.
- [Uerner et al., 2013] Uerner, R., Wulff, S., and Ben-David, S. (2013). Plal: Cluster-based active learning. In *Conference on Learning Theory*, pages 376–397.
- [Viering et al., 2017] Viering, T. J., Krijthe, J. H., and Loog, M. (2017). Nuclear discrepancy for active learning. *arXiv preprint arXiv:1706.02645*.
- [Wang and Ye, 2015] Wang, Z. and Ye, J. (2015). Querying discriminative and representative samples for batch mode active learning. *ACM Transactions on Knowledge Discovery from Data (TKDD)*, 9(3):17.
- [Wasserman, 2019] Wasserman, L. (2019). Lecture note: Statistical methods for machine learning.
- [Weed and Bach, 2017] Weed, J. and Bach, F. (2017). Sharp asymptotic and finite-sample rates of convergence of empirical measures in wasserstein distance. *arXiv preprint arXiv:1707.00087*.
- [Xiao et al., 2017] Xiao, H., Rasul, K., and Vollgraf, R. (2017). Fashion-mnist: a novel image dataset for benchmarking machine learning algorithms.
- [Yin et al., 2017] Yin, C., Qian, B., Cao, S., Li, X., Wei, J., Zheng, Q., and Davidson, I. (2017). Deep similarity-based batch mode active learning with exploration-exploitation. In *2017 IEEE International Conference on Data Mining (ICDM)*, pages 575–584. IEEE.
- [Zhu and Bento, 2017] Zhu, J.-J. and Bento, J. (2017). Generative adversarial active learning. *arXiv preprint arXiv:1702.07956*.

Appendix A Theorem 1: Proof

Theorem 2. *Supposing \mathcal{D} is the data generation distribution and \mathcal{Q} is the querying distribution, if the loss ℓ is symmetric, L -Lipschitz; $\forall h \in \mathcal{H}$ is at most H -Lipschitz function and underlying labeling function h^* is $\phi(\lambda)$ -(\mathcal{D}, \mathcal{Q}) Joint Probabilistic Lipschitz, then the expected risk w.r.t. \mathcal{D} can be upper bounded by:*

$$R_{\mathcal{D}}(h) \leq R_{\mathcal{Q}}(h) + L(H + \lambda)W_1(\mathcal{D}, \mathcal{Q}) + L\phi(\lambda)$$

A.1 Notations

We define the hypothesis $h : \mathcal{X} \rightarrow \mathcal{Y} = [0, 1]$ and loss function $\ell : \mathcal{Y} \times \mathcal{Y} \rightarrow \mathbb{R}^+$, then the expected risk w.r.t. \mathcal{D} is $R_{\mathcal{D}}(h) = \mathbb{E}_{x \sim \mathcal{D}} \ell(h(x), h^*(x))$ and empirical risk $\hat{R}_{\mathcal{D}}(f) = \frac{1}{N} \sum_{i=1}^N \ell(h(x_i), y_i)$. We assume the loss ℓ is symmetric, L -Lipschitz and bounded by M .

A.2 Transfer risk

The first step is to bound the the gap $R_{\mathcal{D}}(h) - R_{\mathcal{Q}}(h)$:

$$\begin{aligned} R_{\mathcal{D}}(h) - R_{\mathcal{Q}}(h) &\leq |R_{\mathcal{D}}(h) - R_{\mathcal{Q}}(h)| = |\mathbb{E}_{x \sim \mathcal{D}} \ell(h(x), h^*(x)) - \mathbb{E}_{x \sim \mathcal{Q}} \ell(h(x), h^*(x))| \\ &= \left| \int_{x \in \Omega} \ell(h(x), h^*(x)) d(\mathcal{D} - \mathcal{Q}) \right| \end{aligned} \quad (12)$$

From the Kantorovich - Rubinstein duality theorem and combining Eq. (12), for **any** distribution coupling $\gamma \in \Pi(\mathcal{D}, \mathcal{Q})$, we have:

$$\begin{aligned} &= \left| \int_{\Omega \times \Omega} (\ell(h(x_{\mathcal{D}}), h^*(x_{\mathcal{D}})) - \ell(h(x_{\mathcal{Q}}), h^*(x_{\mathcal{Q}}))) d\gamma(x_{\mathcal{D}}, x_{\mathcal{Q}}) \right| \\ &\leq \int_{\Omega \times \Omega} |\ell(h(x_{\mathcal{D}}), h^*(x_{\mathcal{D}})) - \ell(h(x_{\mathcal{Q}}), h^*(x_{\mathcal{Q}}))| d\gamma(x_{\mathcal{D}}, x_{\mathcal{Q}}) \\ &\leq \int_{\Omega \times \Omega} |\ell(h(x_{\mathcal{D}}), h^*(x_{\mathcal{D}})) - \ell(h(x_{\mathcal{D}}), h^*(x_{\mathcal{Q}}))| + |\ell(h(x_{\mathcal{D}}), h^*(x_{\mathcal{Q}})) - \ell(h(x_{\mathcal{Q}}), h^*(x_{\mathcal{Q}}))| d\gamma(x_{\mathcal{D}}, x_{\mathcal{Q}}) \end{aligned}$$

Since we assume ℓ is symmetric and L -Lipschitz, then we have:

$$\leq L \int_{\Omega \times \Omega} |h^*(x_{\mathcal{D}}) - h^*(x_{\mathcal{Q}})| d\gamma(x_{\mathcal{D}}, x_{\mathcal{Q}}) + L \int_{\Omega \times \Omega} |h(x_{\mathcal{D}}) - h(x_{\mathcal{Q}})| d\gamma(x_{\mathcal{D}}, x_{\mathcal{Q}}) \quad (13)$$

From Eq.(13) the risk gap is controlled by two terms, the property of labeling function and property of predictor. Moreover, we assume the learner is H -Lipschitz function, then we have:

$$\leq L \int_{\Omega \times \Omega} |h^*(x_{\mathcal{D}}) - h^*(x_{\mathcal{Q}})| d\gamma(x_{\mathcal{D}}, x_{\mathcal{Q}}) + LH \int_{\Omega \times \Omega} \|x_{\mathcal{D}} - x_{\mathcal{Q}}\|_2 d\gamma(x_{\mathcal{D}}, x_{\mathcal{Q}})$$

Labeling function assumption As mentioned before, the goodness of the underlying labeling function decides the level of risk. [Uerner et al., 2013] formalize the such a property as *Probabilistic Lipschitz* condition in AL, in which relaxes the condition of Lipschitzness condition and formalizes the intuition that *under suitable feature representation the probability of two close points having different labels is small* [Uerner and Ben-David, 2013]. We adopt the joint probabilistic Lipschitz property, which is coherent with [Courty et al., 2017].

Definition 2. *The labeling function h^* satisfies $\phi(\lambda)$ -(\mathcal{D}, \mathcal{Q}) Joint Probabilistic Lipschitz if $\text{supp}(\mathcal{Q}) \subseteq \text{supp}(\mathcal{D})$ and for all $\lambda > 0$:*

$$\mathbb{P}_{(x_{\mathcal{D}}, x_{\mathcal{Q}}) \sim \gamma} [|h^*(x_{\mathcal{D}}) - h^*(x_{\mathcal{Q}})| > \lambda \|x_{\mathcal{D}} - x_{\mathcal{Q}}\|_2] \leq \phi(\lambda) \quad (14)$$

Where $\phi(\lambda)$ reflects the decay rate. [Uerner et al., 2013] showed that the faster the decay of $\phi(\lambda)$ with $\lambda \rightarrow 0$, the nicer the distribution and the easier it is to learn the task.

Combining with Eq.(14), the labeling function term can be decomposed and upper bounded by:

$$\begin{aligned} &\leq L \int_{\Omega \times \Omega} \mathbf{1}\{|h^*(x_{\mathcal{D}}) - h^*(x_{\mathcal{Q}})| \leq \lambda \|x_{\mathcal{D}} - x_{\mathcal{Q}}\|_2\} |h^*(x_{\mathcal{D}}) - h^*(x_{\mathcal{Q}})| d\gamma(x_{\mathcal{D}}, x_{\mathcal{Q}}) \\ &+ L \int_{\Omega \times \Omega} \mathbf{1}\{|h^*(x_{\mathcal{D}}) - h^*(x_{\mathcal{Q}})| > \lambda \|x_{\mathcal{D}} - x_{\mathcal{Q}}\|_2\} |h^*(x_{\mathcal{D}}) - h^*(x_{\mathcal{Q}})| d\gamma(x_{\mathcal{D}}, x_{\mathcal{Q}}) \\ &\leq L\lambda \int_{\Omega \times \Omega} \|x_{\mathcal{D}} - x_{\mathcal{Q}}\|_2 d\gamma(x_{\mathcal{D}}, x_{\mathcal{Q}}) + L\phi(\lambda) \end{aligned}$$

The first term is upper bounded through the probability of this event at most 1 and second term adopts the definition of Joint Probabilistic Lipschitz with restricting the output space $h^*(\cdot) \in [0, 1]$. Plugging in the aforementioned results, we have:

$$\leq L(H + \lambda) \int_{\Omega \times \Omega} \|x_{\mathcal{D}} - x_{\mathcal{Q}}\|_2 d\gamma(x_{\mathcal{D}}, x_{\mathcal{Q}}) + L\phi(\lambda)$$

Since this inequality satisfies with any distribution coupling γ , then it is also satisfies with the optimal coupling, w.r.t. the Wasserstein-1 distance with the cost function ℓ_2 distance: $\|\cdot\|_2$. Then we have:

$$R_{\mathcal{D}}(h) - R_{\mathcal{Q}}(h) \leq L(H + \lambda) \inf_{\gamma} \int_{\Omega \times \Omega} \|x_{\mathcal{D}} - x_{\mathcal{Q}}\|_2 d\gamma(x_{\mathcal{D}}, x_{\mathcal{Q}}) + L\phi(\lambda)$$

Finally we can derive:

$$R_{\mathcal{D}}(h) \leq R_{\mathcal{Q}}(h) + L(H + \lambda)W_1(\mathcal{D}, \mathcal{Q}) + L\phi(\lambda) \quad (15)$$

Appendix B Corollary 1: Proof

B.1 Basic statistical learning theory

According to the standard statistical learning theory such as [Mohri et al., 2018], w.h.p. $1 - \delta/2$, $\forall h \in \mathcal{H}$ we have:

$$R_{\mathcal{D}}(h) \leq \hat{R}_{\mathcal{D}}(h) + 2L\text{Rad}_N(h) + \kappa_1(\delta, N) \quad (16)$$

Where $\text{Rad}_N(h) = \mathbb{E}_{S \sim \mathcal{D}^N} \mathbb{E}_{\sigma_1^N} [\sup_h \frac{1}{N} \sum_{i=1}^N \sigma_i h(x_i)]$ is the expected Rademacher complexity with $\text{Rad}_N(h) = \mathcal{O}(\sqrt{\frac{1}{N}})$, and $\kappa_1(\delta, N) = \mathcal{O}(\sqrt{\frac{M \log(2/\delta)}{N}})$ is the confidence term.

In the Active learning, the goal is to control the generalization error w.r.t. (\mathcal{D}, h^*) , thus from Eq.16 we have:

$$R_{\mathcal{D}}(h) \leq (R_{\mathcal{D}}(h) - R_{\mathcal{Q}}(h)) + \hat{R}_{\mathcal{Q}}(h) + 2L\text{Rad}_{N_q}(h) + \kappa_1(\delta, N_q)$$

Combining with Eq.(15), we have

$$R_{\mathcal{D}}(h) \leq \hat{R}_{\mathcal{Q}}(h) + L(H + \lambda)W_1(\mathcal{D}, \mathcal{Q}) + L\phi(\lambda) + 2L\text{Rad}_{N_q}(h) + \kappa_1(\delta, N_q)$$

In general we have finite observations (Supposing we have the sample i.i.d. sampled from query distribution \mathcal{Q}) with Dirac distribution: $\hat{D} = \frac{1}{N} \sum_{i=1}^N \delta\{x_{\mathcal{D}}^i\}$ and $\hat{Q} = \frac{1}{N_q} \sum_{i=1}^{N_q} \delta\{x_{\mathcal{Q}}^i\}$ with $N_q \leq N$. Several recent works show the concentration bound between empirical and expected Wasserstein distance such as [Bolley et al., 2007, Weed and Bach, 2017]. We just adopt the conclusion from [Weed and Bach, 2017] and apply to bound the empirical measures in Wasserstein-1 distance.

Lemma 1. [Weed and Bach, 2017] [Definition 3,4] Given a measure μ on X , the (ϵ, τ) -covering number on a given set $S \subseteq X$ is:

$$\mathcal{N}_{\epsilon}(\mu, \tau) := \inf\{\mathcal{N}_{\epsilon}(S) : \mu(S) \geq 1 - \tau\}$$

and the (ϵ, μ) -dimension is:

$$d_{\epsilon}(\mu, \tau) := \frac{\log \mathcal{N}_{\epsilon}(\mu, \epsilon)}{-\log \epsilon}$$

Then the upper Wasserstein-1 dimensions can be defined as:

$$d_1^*(\mu) = \inf\{s \in (2, +\infty) : \limsup_{\epsilon \rightarrow 0} d_{\epsilon}(\mu, \epsilon^{-\frac{s}{s-2}}) \leq s\}$$

Lemma 2. [Weed and Bach, 2017][Theorem 1, Proposition 20] For $p = 1$ and $s \geq d_1^*(\mu)$, there exists a positive constant C with probability at least $1 - \delta$, we have:

$$W_1(\mu, \hat{\mu}_N) \leq CN^{-1/s} + \sqrt{\frac{1}{2N} \log(\frac{1}{\delta})}$$

Since $s > 2$ thus the convergence rate of Wasserstein distance is slower than $\mathcal{O}(N^{-1/2})$, also named as *weak convergence*. Then according to the triangle inequality of Wasserstein-1 distance, we have:

$$W_1(\mathcal{D}, \mathcal{Q}) \leq W_1(\mathcal{D}, \hat{\mathcal{D}}) + W_1(\hat{\mathcal{D}}, \mathcal{Q}) \leq W_1(\mathcal{D}, \hat{\mathcal{D}}) + W_1(\hat{\mathcal{D}}, \hat{\mathcal{Q}}) + W_1(\hat{\mathcal{Q}}, \mathcal{Q}) \quad (17)$$

Combing the conclusion with Lemma 2, there exist some constants (C_d, s_d) and (C_q, s_q) we have with probability $1 - \delta/2$:

$$W_1(\mathcal{D}, \mathcal{Q}) \leq W_1(\hat{\mathcal{D}}, \hat{\mathcal{Q}}) + C_d N^{-1/s_d} + C_q N_q^{-1/s_q} + \sqrt{\frac{1}{2} \log(\frac{2}{\delta})} (\sqrt{\frac{1}{N}} + \sqrt{\frac{1}{N_q}}) \quad (18)$$

Combining Eq.18 and Eq.16, we have

$$R_{\mathcal{D}}(h) \leq \hat{R}_{\mathcal{Q}}(h) + L(H + \lambda)W_1(\hat{\mathcal{D}}, \hat{\mathcal{Q}}) + L\phi(\lambda) + 2L\text{Rad}_{N_q}(h) + \kappa(\delta, N, N_q)$$

Where $\kappa(\delta, N, N_q) = \mathcal{O}(N^{-1/s_d} + N_q^{-1/s_q} + \sqrt{\frac{\log(1/\delta)}{N}} + \sqrt{\frac{\log(1/\delta)}{N_q}})$

Appendix C Computing \mathcal{H} -divergence and Wasserstein distance

C.1 \mathcal{H} divergence

$d_{\mathcal{H}}(\mathcal{D}_1, \mathcal{D}_3)$ We can discuss the discrepancy with different values of p , since $\mathcal{D}_3 \subseteq \mathcal{D}_1$ then we have $x_0 \in [a + b, 2a - b]$:

1. If $p \leq x_0 - b$, then the area of mis-classification will be $(2a - p) + 2b$. If we select $p = x_0 - b$, then the optimal mis-classification area will be $2a + 2b - x_0 \geq 2a + 2b - 2a + b = 3b$
2. If $p \in [x_0 - b, x_0 + b]$, then the area of mis-classification will be $(2a - p) + (p - (x_0 - b)) = 2a + b - x_0 \geq 2a + b - 2a + b = 2b$
3. If $p \geq x_0 + b$, then the area of mis-classification will be $2b + \max(0, 2a - p)$, if we select $p \geq 2a$, then the optimal mis-classification area will be $2b$.

Then the minimal mis-classification area is $2b$, corresponding the optimal risk $\frac{b}{a+b}$, then $d_{\mathcal{H}}(\mathcal{D}_1, \mathcal{D}_3) = \frac{b}{a+b}$

$d_{\mathcal{H}}(\mathcal{D}_1, \mathcal{D}_2)$ We can discuss the discrepancy with different values of p , since $\mathcal{D}_2 \subseteq \mathcal{D}_1$, then we have $x_0 \in [a + b/2, 2a - b/2]$:

1. If $p \leq -x_0 - b/2$, then the mis-classification area will be $a + \max(0, p + a) + 2b$ with optimal value $2a + b/2 - x_0 + 2b \geq a + 2b$;
2. If $p \in [-x_0 - b/2, -x_0 + b/2]$, then the mis-classification area will be $p - (-x_0 - b/2) + (-a - p) + a + b = x_0 + 3b/2 \geq a + 2b$;
3. If $p \in [-x_0 + b/2, x_0 - b/2]$, then the mis-classification area will be $b + a$;
4. If $p \in [x_0 - b/2, x_0 + b/2]$, then the mis-classification area will be $b + p - (x_0 - b/2) + (2a - p) = 2a + 3b/2 - x_0 \geq 2a + b/2 - 2a + b/2 + b = 2b$
5. If $p \geq x_0 + b/2$, then the mis-classification area will be $2b + \max(0, 2a - p) \geq 2b$

Then the minimal mis-classification area is $2b$, corresponding the optimal risk $\frac{b}{a+b}$, then $d_{\mathcal{H}}(\mathcal{D}_1, \mathcal{D}_2) = \frac{b}{a+b}$.

From the previous example $d_{\mathcal{H}}(\mathcal{D}_1, \mathcal{D}_2) = d_{\mathcal{H}}(\mathcal{D}_1, \mathcal{D}_3)$, we show the \mathcal{H} divergence is not good metric for measuring the representative in the data space. Since we want the query distribution more diverse spread in the space, then \mathcal{H} may not be a good indicator.

C.2 Wasserstein-1 distance

We can also estimate the distribution distance through Wasserstein-1 metric. From [Wasserman, 2019] we have:

$$W_1(P, Q) = \int_0^1 |F^{-1}(z) - G^{-1}(z)| dz$$

where $F(z)$ and $G(z)$ is the CDF (cumulative density function) of distribution P and Q , respectively.

CDF of \mathcal{D}_1 , \mathcal{D}_2 and \mathcal{D}_3

1.

$$F_1(z) = \begin{cases} \frac{1}{2a}(z + 2a) & -2a \leq z \leq -a \\ \frac{1}{2} & -a \leq z \leq a \\ \frac{1}{2a}z & a \leq z \leq 2a \end{cases}$$

$$F_1^{-1}(z) = \begin{cases} 2a(z - 1) & 0 \leq z < 1/2 \\ [-a, a] & z = 1/2 \\ 2az & 1/2 < z \leq 1 \end{cases}$$

2.

$$F_2(z) = \begin{cases} \frac{1}{2b}(z + x_0 + b/2) & -x_0 - b/2 \leq z \leq -x_0 + b/2 \\ \frac{1}{2} & -x_0 + b/2 \leq z \leq x_0 - b/2 \\ \frac{1}{2b}(z - x_0 + 3b/2) & x_0 - b/2 \leq z \leq x_0 + b/2 \end{cases}$$

$$F_2^{-1}(z) = \begin{cases} 2bz - x_0 - b/2 & 0 \leq z < 1/2 \\ [-x_0 + b/2, x_0 - b/2] & z = 1/2 \\ 2bz + x_0 - 3b/2 & 1/2 < z \leq 1 \end{cases}$$

3.

$$F_3(z) = \frac{1}{2b}(z - x_0 + b) \quad z \in [x_0 - b, x_0 + b]$$

$$F_3^{-1}(z) = 2bz + x_0 - b \quad z \in [0, 1]$$

Computing $W_1(\mathcal{D}_1, \mathcal{D}_2)$ According to the definition, we can compute

$$W_1(\mathcal{D}_1, \mathcal{D}_2) = \int_0^{1/2} |2a(z - 1) - 2bz - x_0 - \frac{b}{2}| dz + \int_{1/2}^1 |2az - 2bz - x_0 + \frac{3}{2}b| dz$$

We firstly compute $\int_0^{1/2} |2a(z - 1) - 2bz - x_0 - \frac{b}{2}| dz$, since $2a(z - 1) - 2bz - x_0 - \frac{b}{2} < 0$ for $z \in [0, 1/2]$ (since $-a - b - x_0 - b/2 < 0$). Then we have:

$$\begin{aligned} \int_0^{1/2} |2a(z - 1) - 2bz - x_0 - \frac{b}{2}| dz &= \int_0^{1/2} \{-2a(z - 1) + 2bz + x_0 + \frac{b}{2}\} dz \\ &= \frac{3}{4}a + \frac{1}{2}x_0 + \frac{1}{2}b \end{aligned}$$

Then we compute the second part:

$$\begin{aligned} &\int_{1/2}^1 |2az - 2bz - x_0 + \frac{3}{2}b| dz \\ &= \int_{1/2}^{z_0} \{(x_0 - \frac{3}{2}b) - 2(a - b)z\} dz + \int_{z_0}^1 \{2(a - b)z - x_0 + \frac{3}{2}b\} dz \\ &= \frac{1}{2(a - b)}(x_0 - \frac{3}{2}b)^2 - \frac{3}{2}(x_0 - \frac{3}{2}b) + \frac{3}{4}(a - b) \end{aligned}$$

with $z_0 = \frac{x_0 - 3b/2}{2(a-b)}$. Therefore we can compute the wasserstein-1 distance between distribution \mathcal{D}_1 and \mathcal{D}_2 :

$$= \frac{1}{2(a-b)}(x_0 - \frac{3}{2}b)^2 - x_0 + 2b + \frac{3}{2}a$$

With $x_0 \in [a + b/2, 2a - b/2]$. If we take $x_0 = 2a - b/2$, we can get the maximum:

$$\max_{x_0} W_1(\mathcal{D}_1, \mathcal{D}_2) = \frac{3}{2}a - \frac{b}{2}$$

Computing $W_1(\mathcal{D}_1, \mathcal{D}_3)$ According to definition, we can compute

$$W_1(\mathcal{D}_1, \mathcal{D}_3) = \int_0^{1/2} |2a(z-1) - 2bz - x_0 + b|dz + \int_{1/2}^1 |2az - 2bz - x_0 + b|dz$$

We firstly compute $\int_0^{1/2} |2a(z-1) - 2bz - x_0 + b|dz$, since $2(a-b)z - 2a - x_0 + b \leq 0$ for $z \in [0, 1/2]$. (easy to verify: $2(a-b)z - 2a - x_0 + b \leq (a-b) - 2a - x_0 + b = -a - x_0 < 0$), then

$$\begin{aligned} \int_0^{1/2} |2a(z-1) - 2bz - x_0 + b|dz &= \int_0^{1/2} (x_0 + 2a - b) - 2(a-b)z dz \\ &= \frac{1}{2}(x_0 + 2a - b) - \frac{1}{4}(a-b) = \frac{3}{4}a + x_0 - \frac{1}{4}b \end{aligned}$$

Then we compute the second term $\int_{1/2}^1 |2az - 2bz - x_0 + b|dz$, we define $z_0 = \frac{x_0 - b}{2(a-b)}$ and we can verify that $z_0 \in [1/2, 1]$, then this term can be decomposed as we can rewrite it as:

$$\begin{aligned} \int_{1/2}^{z_0} -2(a-b)z + (x_0 - b)dz + \int_{z_0}^1 2(a-b)z - (x_0 - b)dz \\ = \frac{(x_0 - b)^2}{2(a-b)} - \frac{3}{2}(x_0 - b) + \frac{5}{4}(a-b) \end{aligned}$$

Then $W_1(\mathcal{D}_1, \mathcal{D}_3) = \frac{(x_0 - b)^2}{2(a-b)} - \frac{3}{2}(x_0 - b) + \frac{5}{4}(a-b) + \frac{1}{2}x_0 + \frac{3}{4}a - \frac{b}{4} = \frac{1}{2(a-b)}(x_0 - b)^2 - x_0 + 2a = \frac{1}{2(a-b)}(x_0 - b)^2 - x_0 + 2a$ since $x_0 \in [a + b, 2a - b]$, then we have:

$$\min_{x_0} W_1(\mathcal{D}_1, \mathcal{D}_3) = \frac{(x_0 - b)^2}{2(a-b)} - (a+b) + 2a = \frac{a^2}{2(a-b)} + a - b$$

We can verify: $\frac{a^2}{2(a-b)} + a - b > \frac{3}{2}a - \frac{b}{2}$ when $a > b$, then we have:

$$\min_{x_0} W_1(\mathcal{D}_1, \mathcal{D}_3) > \max_{x_0} W_1(\mathcal{D}_1, \mathcal{D}_2)$$

which means in Wasserstein-1 distance metric, the diversity of two distribution can be much better measured.

Appendix D Developing loss in deep batch active learning

We have the original loss:

$$\min_{\theta^f, \theta^h, \hat{B}} \max_{\theta^d} \mathbb{E}_{(x,y) \sim \hat{L} \cup \hat{B}} \ell(h(x, y)) + \mu(\mathbb{E}_{x \sim \hat{\mathcal{D}}} [g(x)] - \mathbb{E}_{x \sim \hat{L} \cup \hat{B}} [g(x)]). \quad (19)$$

Since \hat{L} , \hat{B} and \hat{D} are Dirac distributions, then we have:

$$\begin{aligned}
 & \frac{1}{L+B} \sum_{(x,y) \in \hat{L} \cup \hat{B}} \ell(h(x,y)) + \mu \left(\frac{1}{L+U} \sum_{x \in \hat{D}} g(x) - \frac{1}{L+B} \sum_{x \in \hat{L} \cup \hat{B}} g(x) \right) \\
 &= \frac{1}{L+B} \sum_{(x,y) \in \hat{L}} \ell(h(x,y)) + \frac{1}{L+B} \sum_{(x,y^?) \in \hat{B}} \ell(h(x,y^?)) \\
 &+ \mu \left(\frac{1}{L+U} \sum_{x \in \hat{L}} g(x) + \frac{1}{L+U} \sum_{x \in \hat{U}} g(x) - \frac{1}{L+B} \sum_{x \in \hat{L}} g(x) - \frac{1}{L+B} \sum_{x \in \hat{B}} g(x) \right) \\
 &= \frac{1}{L+B} \sum_{(x,y) \in \hat{L}} \ell(h(x,y)) + \frac{1}{L+B} \sum_{(x,y^?) \in \hat{B}} \ell(h(x,y^?)) \\
 &+ \mu \left(\frac{1}{L+U} \sum_{x \in \hat{U}} g(x) - \left(\frac{1}{L+B} - \frac{1}{L+U} \right) \sum_{x \in \hat{L}} g(x) - \frac{\mu}{L+B} \sum_{x \in \hat{B}} g(x) \right) \\
 &= \underbrace{\left(\frac{1}{L+B} \sum_{(x,y) \in \hat{L}} \ell(h(x,y)) + \mu \left(\frac{1}{L+U} \sum_{x \in \hat{U}} g(x) - \left(\frac{1}{L+B} - \frac{1}{L+U} \right) \sum_{x \in \hat{L}} g(x) \right) \right)}_{\text{Training Stage}} \\
 &+ \underbrace{\left(\frac{1}{L+B} \sum_{(x,y^?) \in \hat{B}} \ell(h(x,y^?)) - \frac{\mu}{L+B} \sum_{x \in \hat{B}} g(x) \right)}_{\text{Querying Stage}}
 \end{aligned}$$

We note that $x \in \hat{D}$ means enumerating all samples from the observations (empirical distribution).

Appendix E Redundancy trick: Computation

$$\begin{aligned}
 & \mu \left(\frac{1}{L+U} \sum_{x \in \hat{U}} g(x) - \left(\frac{1}{L+B} - \frac{1}{L+U} \right) \sum_{x \in \hat{L}} g(x) \right) \\
 &= \mu \left(\frac{\gamma}{1+\gamma} \frac{1}{U} \sum_{x \in \hat{U}} g(x) - \left(\frac{1}{1+\alpha} - \frac{1}{1+\gamma} \right) \frac{1}{L} \sum_{x \in \hat{L}} g(x) \right) \\
 &= \mu' \left(\frac{1}{U} \sum_{x \in \hat{U}} g(x) - \frac{1}{\gamma} \left(\frac{1+\gamma}{1+\alpha} - 1 \right) \frac{1}{L} \sum_{x \in \hat{L}} g(x) \right) \\
 &= \mu' \left(\frac{1}{U} \sum_{x \in \hat{U}} g(x) - \frac{1}{\gamma} \frac{\gamma - \alpha}{1+\alpha} \frac{1}{L} \sum_{x \in \hat{L}} g(x) \right)
 \end{aligned}$$

Appendix F Uniform Output Arrives the Minimal loss

For the abuse of notation, we suppose the output of classifier $h(x, \cdot) = [p_1, \dots, p_K] \equiv \mathbf{p}$ with $p_i > 0$ and $\sum_{i=1}^K p_i = 1$. Then we tried to minimize

$$\min_{\mathbf{p}} \sum_{i=1}^K -\log p_i$$

By applying the Lagrange Multiplier approach, we have

$$\min_{\mathbf{p}, \lambda > 0} \sum_{i=1}^K -\log p_i + \lambda \left(\sum_{i=1}^K p_i - 1 \right)$$

Then we do the partial derivative w.r.t. p_i , then we have $\forall i$:

$$\frac{-1}{p_i} + \lambda = 0 \rightarrow p_i = \frac{1}{\lambda}$$

Given $\sum_{i=1}^K p_i = 1$, then we can compute $p_i = \frac{1}{K}$ arriving the minimal, i.e the uniform distribution.

Appendix G Experiments

G.1 Dataset Descriptions

Dataset	#Classes	Train + Validation	Test	Initially labelled	Query size	Image size
Fashion-MNIST [Xiao et al., 2017]	10	40K + 20K	10K	1K	500	28×28
SVHN [Netzer et al., 2011]	10	40K + 33K	26K	1K	1K	32×32
CIFAR10 [Krizhevsky et al., 2009]	10	45K + 5K	10K	2K	2K	32×32
STL10* [Coates et al., 2011]	10	8K + 1K	4K	0.5K	0.5K	96×96

Table 2: Dataset descriptions

*We used a variant instead of the original STL10 dataset with arranging the training size to 8K (each class 800) and validation 1K and test 4K. We do not use the unlabeled dataset in our training or test procedure.

G.2 Implementation details

FashionMNIST For the FashionMNIST dataset, we adopted the LeNet5 as feature extractor, then we used two-layer MLPs for the classification (320-50-relu-dropout-10) and critic function (320-50-relu-dropout-1-sigmoid).

SVHN, CIFAR10 We adopt the VGG16 with batch normalization as feature extractor. then we used two-layer MLPs for the classification (512-50-relu-dropout-10) and critic function (512-50-relu-dropout-1-sigmoid).

STL10 We adopt the VGG16 with batch normalization as feature extractor. then we used two-layer MLPs for the classification (4096-100-relu-dropout-10) and critic function (4096-100-relu-dropout-1-sigmoid).

G.3 Hyper-parameter setting

Dataset	lr	Momentum	Mini-Batch size	μ	Selection coefficient	Mixture coefficient**
Fashion-MNIST	0.01*	0.5	64	1e-2	5	0.5
SVHN	0.01*	0.5	64	1e-2	5	0.5
CIFAR10	0.01*	0.3	64	1e-2	10	0.5
STL10	0.01*	0.3	64	1e-3	10	0.5

Table 3: Hyper-parameter setting

* We set the initial learning rate as 0.01, then at 50% epoch we decay to 1e-3, after 75% epoch we decay to 1e-4.

** The mixture coefficient means the convex combination coefficient in the two uncertainty based approach.

G.4 Detailed results with numerical values

We report the accuracy in the form of percentage (%), showing in Tab. 4, 5, 6, 7.

Appendix H Ablation study

In this part, we will conduct \mathcal{H} -divergence based adversarial training for the parameters of DNN.

$$\min_{\theta^f, \theta^h} \max_{\theta^d} \sum_{(x,y) \in \hat{L}} \ell(h(x,y)) - \mu \left(\sum_{x \in \hat{U}} \log(g(x)) + \sum_{x \in \hat{L}} \log(1 - g(x)) \right) \quad (20)$$

Where the g is defined as the discriminator function ⁵. In the adversarial training, the discriminator parameter aims at discriminating the empirical unlabeled and labeled data via the binary classification, while the feature extractor parameter aims at not being correctly classified. By this manner, the unlabeled dataset will be used for constructing a better feature representation in the adversarial training. As for the query part, we directly used baseline strategies. The numerical values will show in Tab. 8. Moreover, we also evaluated the ablation study for the SVHN dataset, showing in Tab. 9 and Fig. 5.

⁵This notation is slightly different from the critic function [Arjovsky et al., 2017]

Deep Active Learning: Unified and Principled Method for Query and Training

	Random	LeastCon	Margin	Entropy	KMedian	DBAL	Core-set	DeepFool	WAAL
1K	58.03±2.81	57.93±1.62	57.81±2.19	57.40±1.75	57.62±2.5	58.01±2.75	58.14±2.19	58.19±2.4	72.29±1.16
1.5K	66.81±1.02	64.24±2.49	65.61± 2.5	66.37±0.62	67.13±2.87	66.53±2.5	68.79±1.99	66.21±1.78	76.99±1.05
2K	71.21±2.35	68.36±1.09	70.05±2.77	69.70±0.88	71.57±0.79	69.77±0.93	71.22±1.38	70.14±1.32	79.85±0.49
2.5K	73.12±2.1	71.68±1.67	72.74±1.55	71.60±1.42	73.84±0.98	72.60±0.60	72.61±1.16	71.77±1.49	81.08±0.68
3K	75.80±0.64	75.03±1.56	76.55±1.01	74.84±1.29	75.79±0.44	74.75±1.04	73.77±1.74	73.69±1.21	82.04±0.58
3.5K	77.34±0.67	77.73±1.04	78.99±1.11	76.66±1.26	77.44±0.97	75.86±1.02	75.10±1.11	74.00±0.71	82.74±0.79
4K	78.68±0.41	79.26±0.47	81.77±0.51	79.00±0.24	77.97±0.65	77.02±0.42	76.28 ±0.98	74.93±2.05	83.25±0.62
4.5K	79.58±0.47	80.08±0.82	82.32±0.47	79.89±0.78	79.49±0.7	77.90±0.58	77.30±0.61	76.64±0.97	83.96±0.54
5K	80.02±0.45	81.32±0.64	83.89±0.84	80.85±0.87	79.97±0.59	78.87±0.58	78.34±0.37	77.24±0.69	84.45±0.45
5.5K	80.93±0.33	83.21±0.42	84.87±0.18	82.26±0.77	81.11±0.41	79.47±2.9	78.42±0.66	77.72±0.57	85.20±0.44
6K	81.30±0.25	84.50±0.73	85.52±0.27	83.66±0.98	81.86±0.6	80.43±0.76	79.66±0.34	78.99±0.33	85.99±0.43

Table 4: Result of FashionMNIST (Average ± std)

	Random	LeastCon	Margin	Entropy	KMedian	DBAL	Core-set	DeepFool	WAAL
1K	63.97±2.04	63.40±2.16	63.10±2.3	63.49±2.79	63.50±2.53	63.76±0.73	63.90±1.07	63.62±2.34	75.18±1.41
2K	75.85±1.16	74.86±2.44	75.27± 1.7	72.78±3.15	76.17±3.2	77.07±1.57	77.9±1.25	76.29±1.62	80.69±2.00
3K	80.83± 1.04	81.87± 0.64	80.9± 2.22	80.88± 1.26	81.36± 1.29	81.17± 1.72	81.7 ± 0.84	80.92± 0.79	83.89± 2.08
4K	82.70±1.18	84.00±0.88	83.10±1.38	83.19±0.95	83.41±1.58	83.95±1.87	84.81±1.3	83.79±0.64	86.82±1.11
5K	85.10±0.73	85.68±0.94	85.02±1.1	84.75±0.83	84.93±0.94	86.34±1.1	86.52±0.95	85.32±0.58	88.71±1.08
6K	86.20±0.48	87.23±0.97	87.53±0.63	87.51±0.50	87.04±0.45	87.61±0.72	88.00 ±0.44	87.02±0.64	89.71±0.83

Table 5: Result of SVHN (Average ± std)

	Random	LeastCon	Margin	Entropy	KMedian	DBAL	Core-set	DeepFool	WAAL
2K	46.33±3.18	46.43±3.17	46.69±3.87	46.79±3.62	46.53±3.39	46.48±3.11	46.38±4.03	46.54±3.77	55.00±0.40
4K	56.33±3.40	53.26±3.84	55.52± 2.69	53.13±2.99	53.58±2.57	56.18±2.37	56.09±3.89	54.48±1.62	62.32±0.36
6K	59.63± 4.17	59.00± 2.19	63.05± 1.78	62.63± 1.29	61.25±1.76	62.48± 1.38	59.56 ± 1.17	60.80± 0.70	66.67± 0.60
8K	62.85±3.37	66.46±1.33	66.44±1.85	65.23±1.89	63.73±1.34	65.84±0.78	65.84±1.27	64.87±1.98	69.33±1.47
10K	68.13±2.53	68.91±1.10	69.86±0.24	69.72±1.53	68.92±2.33	68.94±1.96	69.11±0.80	69.39±0.47	72.39±1.21
12K	70.41±1.02	71.90±1.35	72.25±0.68	71.58±0.77	72.65±0.64	72.25±1.24	72.60 ±0.79	71.17±1.03	75.11±0.49

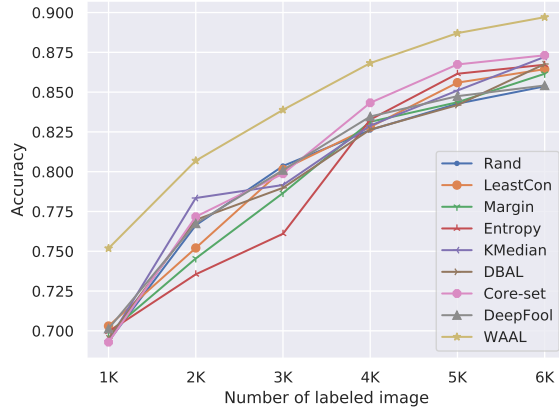
Table 6: Result of CIFAR10 (Average ± std)

	Random	LeastCon	Margin	Entropy	KMedian	DBAL	Core-set	DeepFool	WAAL
0.5K	41.78±2.42	41.69±3.22	41.81±2.27	41.12±1.67	41.24±1.41	41.30±1.45	41.41±2.30	41.82±2.67	47.01±1.09
1K	48.24±1.37	47.05±1.42	46.7±0.85	46.38±2.31	46.45±1.11	47.45±3.71	47.58±2.06	45.15±0.74	52.47±1.62
1.5K	51.78± 2.5	50.87± 1.24	50.44± 2.57	50.24± 1.21	49.91±1.74	52.53± 1.29	51.2 ± 1.63	48.64± 2.43	57.25± 1.78
2K	56.52±1.78	56.25±1.58	55.54±1.09	55.15±2.13	54.92±2.19	57.54±1.70	58.13±1.57	54.26±2.40	60.08±1.63
2.5K	58.42±1.42	58.49±2.05	57.62±1.42	57.81±2.87	57.87±1.51	59.25±2.89	57.66±1.79	57.05±2.53	62.58±1.44
3K	61.13±1.67	60.80±2.64	59.42±1.49	60.88±0.72	60.00±0.65	62.11±1.65	61.02 ±0.48	59.74±1.74	65.42±1.33

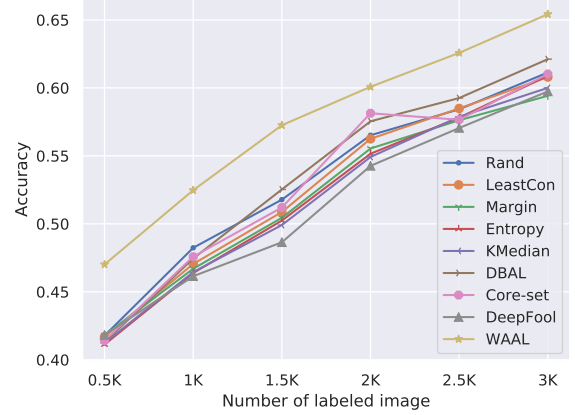
Table 7: Result of STL10 (Average ± std)

	Random	LeastCon	Margin	Entropy	KMedian	DBAL	Core-set	DeepFool	WAAL
2K	49.85±0.32	50.00±1.81	49.8±2.28	49.92±1.08	49.31±2.76	49.58±1.05	49.87±4.03	49.85±1.36	55.00±0.40
4K	56.63±3.27	59.11±0.85	61.93± 2.12	59.15±0.41	60.6±0.72	58.55±1.99	60.97±1.62	58.80±2.59	62.32±0.36
6K	62.30± 2.54	63.15± 2.21	63.04± 1.98	63.74± 0.94	64.73±1.37	63.82± 2.33	64.95 ± 1.66	64.80± 1.4	66.67± 0.60
8K	66.97±0.76	64.32±2.58	68.30±1.02	67.67±1.04	65.98±1.45	66.65±1.00	67.54±2.16	67.65±1.27	69.33±1.47
10K	69.23±1.97	69.74±2.52	69.98±0.25	69.92±1.17	70.95±1.93	69.96±1.74	70.62±0.74	70.55±0.80	72.39±1.21
12K	71.78±1.34	71.60±1.25	71.56±1.53	72.90±1.37	72.56±1.39	73.53±1.71	71.83 ±1.20	71.86±0.33	75.11±0.49

Table 8: Ablation study of CIFAR10 (Average ± std)



(a)



(b)

Figure 5: (a) Ablation study in SVHN: the baselines are all trained by leveraging the unlabeled information through \mathcal{H} -divergence; (b) Empirical performance on STL10, over five repetitions.

	Random	LeastCon	Margin	Entropy	KMedian	DBAL	Core-set	DeepFool	WAAL
1K	68.34 \pm 0.96	70.3 \pm 1.75	68.88 \pm 1.19	68.94 \pm 1.17	68.38 \pm 0.92	68.54 \pm 3.65	69.29 \pm 0.71	70.14 \pm 1.84	75.18 \pm 1.41
2K	76.63 \pm 3.14	75.21 \pm 2.45	74.55 \pm 3.16	73.55 \pm 2.49	78.35 \pm 1.63	76.97 \pm 1.19	77.17 \pm 1.8	76.74 \pm 2.15	80.69 \pm 2.00
3K	80.36 \pm 0.46	80.14 \pm 1.66	78.66 \pm 1.54	76.10 \pm 1.46	79.16 \pm 1.47	78.99 \pm 1.57	79.87 \pm 0.33	80.10 \pm 1.27	83.89 \pm 2.08
4K	82.62 \pm 1.15	82.81 \pm 0.66	83.13 \pm 1.01	83.27 \pm 0.18	82.89 \pm 0.73	82.65 \pm 1.61	84.33 \pm 0.72	83.47 \pm 0.74	86.82 \pm 1.11
5K	84.27 \pm 0.77	85.59 \pm 0.74	84.36 \pm 0.75	86.15 \pm 0.23	85.10 \pm 0.57	84.18 \pm 0.25	86.74 \pm 0.34	84.75 \pm 0.57	88.71 \pm 1.08
6K	85.36 \pm 0.36	86.44 \pm 0.93	86.15 \pm 0.89	86.72 \pm 0.66	87.21 \pm 0.52	86.77 \pm 1.26	87.31 \pm 0.71	85.42 \pm 0.55	89.71 \pm 0.83

Table 9: Ablation study of SVHN (Average \pm std)